



Effective sorption of selenite by Fe–Mn binary oxide: influence of preparation method

Xiaohu Wen^{a,b}, Gaosheng Zhang^{c,*}

^aKey Laboratory of Ecohydrology of Inland River Basin, Chinese Academy of Sciences, Donggang West Rd 320, Lanzhou, 730000, Gansu Province, China, Tel. +86 0931 4967153; email: xhwen@lzb.ac.cn

^bNorthwest Institute of Eco-Environment and Resources, Chinese Academy of Sciences, Donggang West Rd 320, Lanzhou, 730000, Gansu Province, China

^cCollaborative Innovation Center of Water Quality Safety and Protection in Pearl River Delta, Guangzhou University, Guangzhou 510006, China, Tel. +86 020 39366505; emails: zgs77@126.com, gs Zhang@yic.ac.cn (G. Zhang)

Received 1 June 2017; Accepted 23 December 2017

ABSTRACT

In this study, two Fe–Mn binary oxide sorbents with a same Mn:Fe molar ratio of 1:3 were prepared using two methods (coprecipitation and mechanical mixing), and they are denoted as ‘Fe–Mn and ^mFe–Mn, respectively. Both ^mFe–Mn and ‘Fe–Mn are amorphous and have similar structure with 2-line ferrihydrite. The ‘Fe–Mn has a much higher specific surface area than the ^mFe–Mn. Selenite sorption on both ^mFe–Mn and ‘Fe–Mn is pH dependent, decreasing with an increase in pH value. The estimated maximal sorption capacity of Se(IV) on the ^mFe–Mn and ‘Fe–Mn is 48.6 and 70.5 mg/g at pH 7.0, respectively. In addition, the Fe–Mn binary oxide is able to adsorb selenite in the presence of competing anions and across a wide range of pH values. Among the co-existing anions, phosphate is the greatest competitor for adsorptive sites on the surface of oxide. Selenite may be sorbed onto the surface of the Fe–Mn binary oxide by formation of inner-sphere surface complexes. The high sorption capacity, low cost and environmental friendliness of the Fe–Mn binary oxide make it a potentially attractive sorbent for the removal of Se(IV) from water.

Keywords: Fe–Mn binary oxide; Coprecipitation; Mechanical mixing; Selenite; Sorption

1. Introduction

Although selenium is an essential micronutrient for animals and humans, it will lead to serious health risks if taken in excess [1–3]. Some studies showed that excessive amounts of selenium could damage body tissues and organs, and consequently cause deleterious effects such as lower reproduction rates and an increase in birth defects over time [4,5]. Food is the most important route of humans’ exposure to selenium [2], but ingestion of Se from drinking water cannot be neglected even at low concentrations [3,6]. To abate health problems associated with selenium in drinking water, the World Health Organization (WHO) recommended a limit

of 10 µg L⁻¹ as the maximum permissible selenium level. Recently, this standard has been employed by European Commission and China. Taking into account the evidence of increased risk of chronic disease due to long-term exposure, a much more stringent standard of 1 µg L⁻¹ has recently been proposed [7].

Selenium occurs predominantly in two inorganic forms as oxyanions of selenate (SeO₄²⁻) and selenite (HSeO₃⁻, SeO₃²⁻) in water [8]. Selenite is present in mildly oxidizing and neutral pH environments, and more toxic and mobile than selenate [5,9]. Various treatment techniques such as membrane filtration, anion exchange, adsorption and chemical oxidation/reduction have been used for selenium removal from contaminated waters [5,6,10–13]. Among them, adsorption is regarded as one of the most promising methods for selenium removal from water, due to its simplicity, high

* Corresponding author.

efficiency and cost-effectiveness [5]. A large number of adsorbents including natural and synthetic ones have been tested to remove selenium from water or wastewater [6,14–16]. Recently, adsorbents of metal (hydr)oxides have attracted increasing attention. For examples, various iron oxides [17], aluminum oxide [18], titanium oxide [19], manganese oxide [20], MnFe_2O_4 [21] and magnetite [22], have been examined for selenium adsorption.

Compared with individual metal (hydr)oxides, bimetal and trimetal (hydr)oxides usually demonstrate more-attractive adsorptive properties [23] and have recently been gaining popularity in water and wastewater treatment [24–27]. In our previous studies [28,29], a novel Fe(III)–Mn(IV) binary oxide was developed to adsorb arsenic from water. Our studies indicated that the Fe–Mn binary oxide was more effective in arsenic immobilization than either the pure Fe oxide or Mn oxide. In addition, the Fe–Mn binary oxide exhibited high performance in removing oxyanions of phosphate and antimony [30,31]. It can be anticipated that the Fe–Mn binary oxide may be also effective for selenium adsorption due to the similarity of molecular structure between selenium and arsenic. However, to our best knowledge, few studies have been reported in literatures on selenium sorption by Fe–Mn binary oxides. Szlachta et al. [23] synthesized a Fe–Mn oxide adsorbent via a hydrothermal approach, which showed a high adsorptive capacity towards selenite (up to 29.0 mg/g). This adsorbent was composed of MnCO_3 and Fe_2O_3 crystalline phases as well as amorphous phases of Fe(III) and Mn(III) hydrous oxides [23]. However, high temperature and high pressure are required in hydrothermal synthesis, which will increase the fabrication cost of sorbents. Hence, from economic point of view, some simple synthesis methods which can be carried out at ambient conditions, for example, coprecipitation and mechanical mixing, are also more desirable. The adsorption performance of an adsorbent is usually determined by its surface morphology and surface charge, which are significantly affected by synthesis method. Therefore, it is necessary to fully characterize the Fe(III)–Mn(IV) binary oxides synthesized via different methods.

Hence, in this study coprecipitation and mechanical mixing were employed to synthesize Fe–Mn binary oxides, which can be easily operated in kilogram-scale or ton-scale. The main objectives of this research were (1) to characterize the prepared Fe–Mn binary oxides with a variety of techniques; (2) to evaluate their selenite adsorption capacity and investigate sorption kinetics as well as the influences of solution pH and co-existing ions, and finally (3) to analyze the change of surface after selenite sorption.

2. Materials and methods

2.1. Materials

All chemicals are analytical grade and used without further purification. Reaction vessels (glass) were cleaned with 1% HNO_3 and rinsed several times with deionized water before use. Se(IV) stock solution was prepared with deionized water using Na_2SeO_3 . Se(IV) working solutions were freshly prepared by diluting selenite solutions with deionized water.

2.2. Fe–Mn binary oxide preparation

The Fe–Mn binary oxide with a Mn:Fe molar ratio of 1:3 was prepared at ambient room temperature, according to a slightly modified method reported by Zhang et al. [28]. Potassium permanganate (KMnO_4 , 0.015 mol) and iron(II) sulfate heptahydrate ($\text{FeSO}_4 \cdot 7\text{H}_2\text{O}$, 0.045 mol) were dissolved in 200 mL of deionized water, respectively. Under vigorous magnetic stirring, the FeSO_4 solution was added into the KMnO_4 solution simultaneously with 3 M NaOH solution to keep the solution pH in a range between 7 and 8. After addition, the formed suspension was continuously stirred for 1 h, aged at room temperature for 4 h then washed repeatedly with deionized water until no sulfate could be detected. The suspension was then filtrated and dried at 65°C for 24 h. The dry material was crushed and stored in a desiccator for later use. The obtained Fe–Mn binary oxide is denoted as ‘Fe–Mn oxide’. In addition, a mixture of amorphous Fe-oxide and Mn-oxide with a Mn/Fe molar ratio of 1:3 was obtained by a mixing process. The amorphous iron oxide was prepared using the following method: contacting 0.5 M FeCl_3 with 1 M NaOH, the formed suspension was continuously stirred for 1 h, aged at room temperature for 2 h. Suspension of MnO_2 was prepared according to the procedure described by Murray [32]. The obtained MnO_2 suspension was then treated in the same way as that of the amorphous iron oxide. After that, the iron oxide suspension and MnO_2 suspension were combined by rapid mixing and were continuously stirred for 1 h. The following treatment steps were the same as those of ‘Fe–Mn oxide preparation processes. The obtained Fe–Mn binary oxide is denoted as ‘‘Fe–Mn oxide’. The average particle size of the crushed adsorbents was about 30 μm .

2.3. Characterization

X-ray diffraction patterns of powder samples from Fe–Mn binary oxides were obtained using a D/Max-3A diffractometer with Ni-filtered copper $\text{K}\alpha$ radiation. Specific surface area, pore volume and pore size distribution were measured by nitrogen adsorption–desorption isotherm using the Brunauer–Emmett–Teller (BET) method with an ASAP 2000 surface area analyzer (Micromeritics, USA). The morphology of the particles was characterized by a high-resolution transmission electron microscope (TEM, JEM-2100, JEOL, Japan). X-ray photoelectron spectra were collected on an ESCA-Lab-220i-XL spectrometer with a monochromatic Al $\text{K}\alpha$ X-ray source (1,486.6 eV). C1s peaks were used as an inner standard calibration peak at 284.7 eV. For wide scan spectra, an energy range of 0 to 1,100 eV was used with pass energy of 80 eV and step size of 1 eV. The high-resolution scans were conducted according to the peak being examined with pass energy of 40 eV and step size of 0.05 eV. The XPS results were collected in binding energy forms and fitted using a nonlinear least-square curve fitting program (XPSPEAK41 Software).

A Zeta potential analyzer (Zetasizer 2000, Malvern, UK) was used to analyze the Zeta potential of Fe–Mn binary oxide before and after selenite adsorption. The content of the Fe–Mn binary oxide in the solution is about 0.2 g L^{-1} and Se(IV) concentration is 10 mg L^{-1} . 0.01 M NaNO_3 was used as background electrolyte to maintain an approximately constant ionic strength. After adsorption equilibrium, 20 mL of

Fe–Mn binary oxide suspension was transferred to a sample tube. Zeta potential of the suspension was then measured by electrokinetic analysis.

2.4. Batch adsorption

For sorption kinetics, defined amount of selenite stock solution was added in a 1,000-mL glass vessel containing 1,000 mL 0.01 M NaNO₃ solution, to make 7.4 mg/L of initial selenite concentration. The solution pH was adjusted to 7.0 ± 0.1 by adding 0.1 M HNO₃ and/or NaOH and then the Fe–Mn binary oxide was added to obtain a 0.2 g/L suspension. The suspension was mixed by magnetic stirring for 36 h, and the pH was maintained at 7.0 ± 0.1 throughout the experiment by addition of the acid and base solutions. In the whole process, only several drops of acid or base were added into the solution and the total volume was no more than 0.5 mL, which did not significantly influence the selenite sorption. Approximately 5 mL aliquots were taken from the suspension at certain time intervals. The samples were filtered through a 0.45 μm membrane filter and analyzed for selenium.

Adsorption isotherms of selenite on two Fe–Mn binary oxides were obtained using batch experiments at pH 7.0. Initial selenite concentration varied from 5 to 40 mg/L. In each test, 10 mg of the adsorbent sample was loaded in the 150-mL glass vessel and 50 mL of solution containing different amounts of selenite were then added to the vessel. In order to keep the pH level around 7.0, 0.1 M of NaOH or HNO₃ was added, accordingly. The vessels were shaken on an orbit shaker at 140 rpm for 36 h at 25°C ± 1°C. After the reaction period, all samples were filtered by a 0.45 μm membrane filter and analyzed for selenium.

To investigate the influence of pH and ionic strength on the selenite sorption, experiments were carried out by adding 10 mg of the adsorbent sample into 150-mL glass vessels, containing 50 mL of 7.4 mg/L selenite solution. The ionic strength of the solutions varied from 0.005 to 0.5 M by adding NaNO₃. The pH of the solutions was adjusted every 4 h with dilute HNO₃ or/and NaOH solution to designated values in the range of 3–11 during shaking process. The equilibrium pH was measured and the supernatant was filtered through a 0.45 μm membrane after the solutions were mixed for 36 h. Then, the residual selenite concentration in the supernatant solutions was determined.

The influence of commonly co-existing anions in water such as chlorine, fluoride, sulfate, bicarbonate, silicate and phosphate on the removal of selenite was investigated by adding sodium chloride, sodium fluoride, sodium sulfate, sodium bicarbonate, sodium silicate and sodium phosphate to 0.094 mmol/L of selenite solution, respectively. The anion concentrations ranged from 0.1 to 5 mmol/L. The solution pH was adjusted to 7.0 ± 0.1. A defined amount (10 mg) of Fe–Mn binary oxide was added and the solutions were agitated at 140 rpm for 36 h at 24°C ± 1°C. After filtration by a 0.45 μm membrane filter, the concentration of residual selenium was analyzed using ICP–AES.

2.5. Analytical methods

Selenium concentrations were determined using an inductively coupled plasma atomic emission spectroscopy

(ICP–AES, Optima 7100 DV, PerkinElmer Co., USA) machine. Prior to analysis, the aqueous samples were acidified with concentrated HNO₃ in an amount of 1%, and stored in acid-washed glass vessels.

3. Results and discussion

3.1. Characterization of Fe–Mn binary oxide

The chemical analysis of synthesized Fe–Mn binary oxide showed that the Mn:Fe molar ratio of the bulk was 0.336, which is very close to the theoretical value of 1:3. Fig. S1 demonstrates the X-ray diffraction patterns of the synthetic Fe–Mn binary oxides. The pattern of ⁴⁵Fe–Mn is almost identical to that of the ⁵⁵Fe–Mn. Obviously, the two Fe–Mn binary oxides synthesized via coprecipitation or mechanical mixing exist mainly in amorphous phase. Their patterns are very similar to these of poorly ordered 2-line ferrihydrite which has two broad peaks at 34.4° and 62.1°, according to *d* spacing of 0.260 and 0.149 nm, respectively [33,34].

The results of BET specific surface area of the two synthesized Fe–Mn binary oxides are summarized in Table S1. The specific surface area of pure amorphous FeOOH and MnO₂ is 247 and 121 m² g⁻¹, respectively. And the specific surface area of the ⁵⁵Fe–Mn is 219 m² g⁻¹, which is very close to the theoretically calculated value of 216 m² g⁻¹ based on their weight ratio. However, the ⁴⁵Fe–Mn has a higher specific surface area than the ⁵⁵Fe–Mn, being 265 m² g⁻¹. This indicates that coprecipitation creates smaller particles and extra aggregated pores in Fe–Mn binary oxide, which may benefit its adsorption capacity. The TEM images of the ⁴⁵Fe–Mn and ⁵⁵Fe–Mn are shown in Fig. 1. Obviously, the ⁴⁵Fe–Mn grains are aggregated of smaller nanosized particles with uniform shape, and the average size of these nanoparticles is around 20–30 nm. However, the image of ⁵⁵Fe–Mn is remarkably different from that of ⁴⁵Fe–Mn. It seems that the MnO₂ nanoparticles cover mostly the surfaces of amorphous FeOOH nanoparticles.

3.2. Sorption kinetics

Fig. 2(a) depicts the change of adsorbed selenite as a function of contact time. Selenite adsorption process can be divided into two steps as shown in Fig. 2(a). In the first step, the adsorption is rather rapid and over 92% of the equilibrium adsorption capacity is achieved within 2 h. However, the adsorption becomes very slow after 2 h in the second step. To ensure a complete sorption, the contact time was therefore maintained as 36 h for all batch experiments. Sorption solely due to electrostatic processes is usually very rapid, in the order of seconds [35]. The adsorption of selenite on the Fe–Mn binary oxide takes several hours, indicating that a specific adsorption may occur between the selenite and the surface of the oxide [24].

Both pseudo-first-order model and pseudo-second-order model were used to fit the kinetic data of selenite sorption onto the Fe–Mn binary oxide. The mathematical representations of the models are given in Eqs. (1) and (2), respectively:

$$\ln(q_e - q_t) = \ln q_e - k_1 t \text{ (linear form)} \quad (1)$$

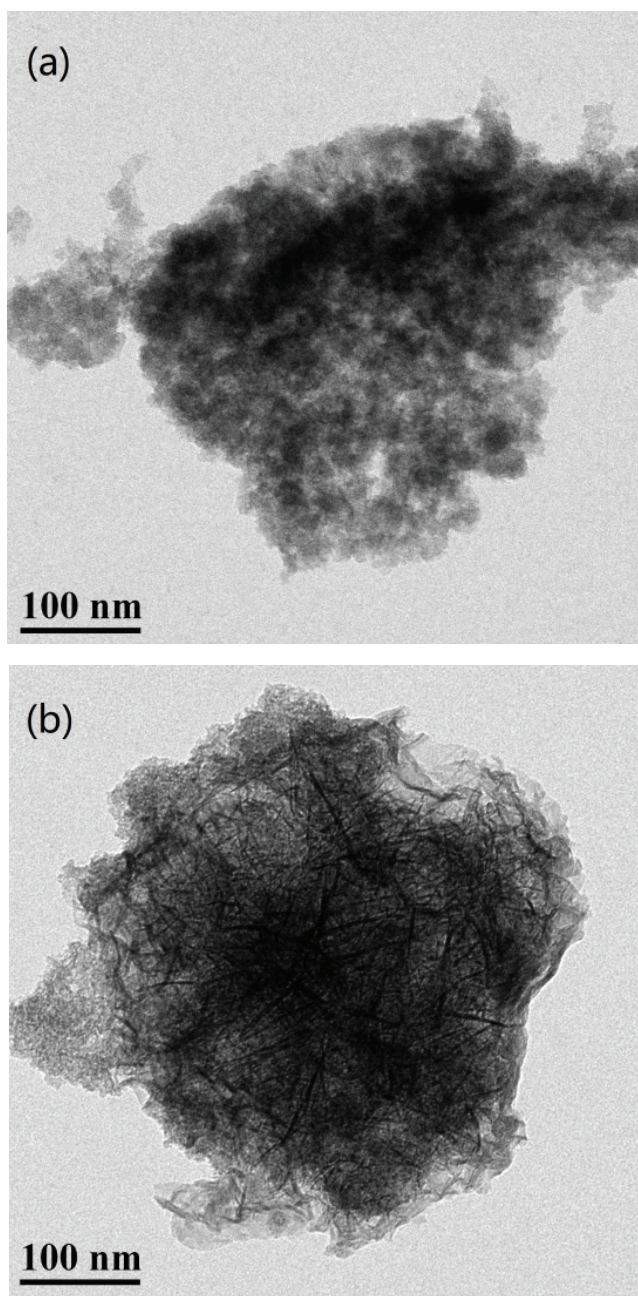


Fig. 1. TEM images of $^{\circ}\text{Fe-Mn}$ (a) and $^{\text{m}}\text{Fe-Mn}$ (b).

$$\frac{t}{q_i} = \frac{1}{k_2 q_e^2} + \frac{1}{q_e} t \quad (\text{linear form}) \quad (2)$$

where q_e and q_i are the adsorption capacities (mg/g) of the adsorbent at equilibrium and at any time, t (h), respectively; k_1 (h^{-1}) and k_2 (g mg/h) are the related adsorption rate constants.

The fitting results are shown in Figs. 2(b) and (c), respectively. In addition, the determination coefficients (r^2) and rate constants obtained from pseudo-first-order and pseudo-second-order models are listed in Table 1. It can be clearly seen that the pseudo-second-order model better fits the experimental data than the pseudo-first-order model.

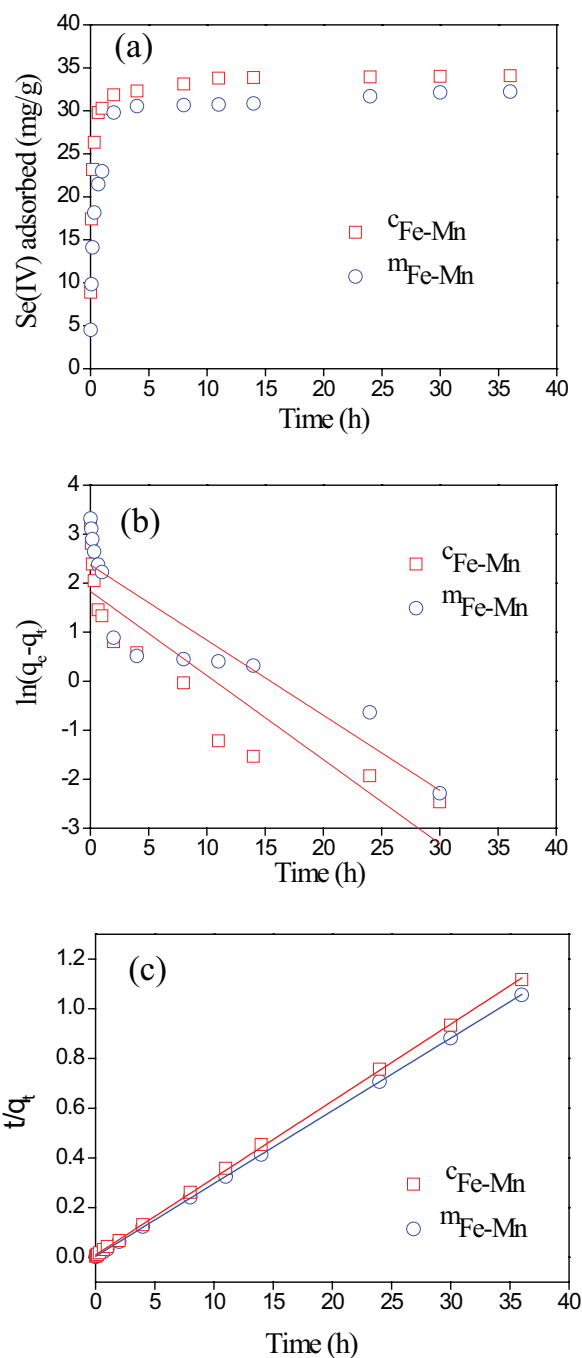


Fig. 2. Sorption kinetics of Se(IV) sorption on $^{\circ}\text{Fe-Mn}$ and $^{\text{m}}\text{Fe-Mn}$. (a) Amount of sorbed Se(IV) vs. contact time, (b) fitted with pseudo-first-order linear equation and (c) fitted with pseudo-second-order linear equation. $[\text{Se(IV)}]$ initial = 7.4 mg/L, adsorbent dose = 200 mg/L, pH = 7.0 ± 0.1 , $T = 25^\circ\text{C} \pm 1^\circ\text{C}$.

A larger adsorption rate constant usually represents a quicker adsorption. From Table 1, it is evident that the sorption rate of selenite on $^{\circ}\text{Fe-Mn}$ is much higher than that of $^{\text{m}}\text{Fe-Mn}$. This quicker removal of selenite by $^{\circ}\text{Fe-Mn}$ may be ascribed to the availability of more adsorptive sites on the surface of $^{\circ}\text{Fe-Mn}$, evidenced by the fact that the $^{\circ}\text{Fe-Mn}$ has a higher specific surface area.

Table 1
Adsorption rate constant obtained from pseudo-first-order model and pseudo-second-order model

Adsorbent	Pseudo-first-order model			Pseudo-second-order model		
	k_1 (h ⁻¹)	q_e (mg/g)	r^2	k_2 (g/mg·h)	q_e (mg/g)	r^2
^m Fe–Mn	0.172	6.2	0.802	0.102	32.4	
^c Fe–Mn	0.153	10.7	0.810	0.237	34.2	

To examine the applicability of ^cFe–Mn for trace selenite removal from water, sorption kinetic of selenite was also investigated at an initial concentration of 150 µg/L. Fig. S2 demonstrates the residual concentration of Se(IV) with the increase of treatment time. It was found that the ^cFe–Mn was rather effective for trace selenite removal. The residual Se(IV) concentration dropped to less than 10 µg/L within 4 min treatment, meeting the WHO standard for Se in drinking water. This suggested that the ^cFe–Mn was feasible to be used for Se removal in real water treatment.

3.3. Sorption edges and ionic strength influence on Se(IV) sorption

From Figs. 3(a) and (b), it can be found that Se(IV) sorption is strongly dependent on pH and decreases with an increase in solution pH. Typically, adsorption of acid anions by metal oxides and hydroxides decreases with an increasing pH [36]. Similar phenomena were also observed for the sorption of Se(IV) onto iron oxides [37,38]. This can be explained by a combination of both chemical and electrostatic effects [39]. Under the tested pH range (3–11), HSeO₃⁻ and SeO₃²⁻ are major Se(IV) species in the solution. Lower pH benefits for the protonation of metal oxide surface. Increased protonation is thought to increase the positively charged sites, which enlarges the attraction force existing between the sorbent surface and selenite anions and therefore increases the amount of sorption in the lower pH region [24]. With the increase in solution pH, the negatively charged sites gradually dominate so that the repulsion effect increases, which inhibits the adsorption of Se(IV). Moreover, there is still a significant amount of Se(IV) sorbed onto Fe–Mn binary oxide at pH values greater than the pH_{IEP} (6.1), where the surface is negatively charged. This indicates that the chemical interaction is involved and dominates the adsorption of Se(IV) at pH above the value of the pH_{IEP}.

Anions adsorbed through outer-sphere association are strongly sensitive to ionic strength and their adsorption is obviously suppressed by competition with weakly adsorbing anions such as NO₃⁻ [24]. Conversely, anions adsorbed by inner-sphere association either show little sensitivity to ionic strength or respond to higher ionic strength with greater adsorption [40]. Ionic strength increase from 0.005 to 0.5 M had no significant effect on Se(IV) sorption (Figs. 4(a) and (b)). Similar observations have also been reported for maghemite [3], hematite [41], goethite and amorphous iron oxyhydroxides [42]. This indicates that Se(IV) is mainly adsorbed by inner-sphere complexation.

3.4. Sorption isotherm

Fig. 4 shows the sorption isotherms of Se(IV) on the ^cFe–Mn and ^mFe–Mn. It can be clearly seen from the figure that both

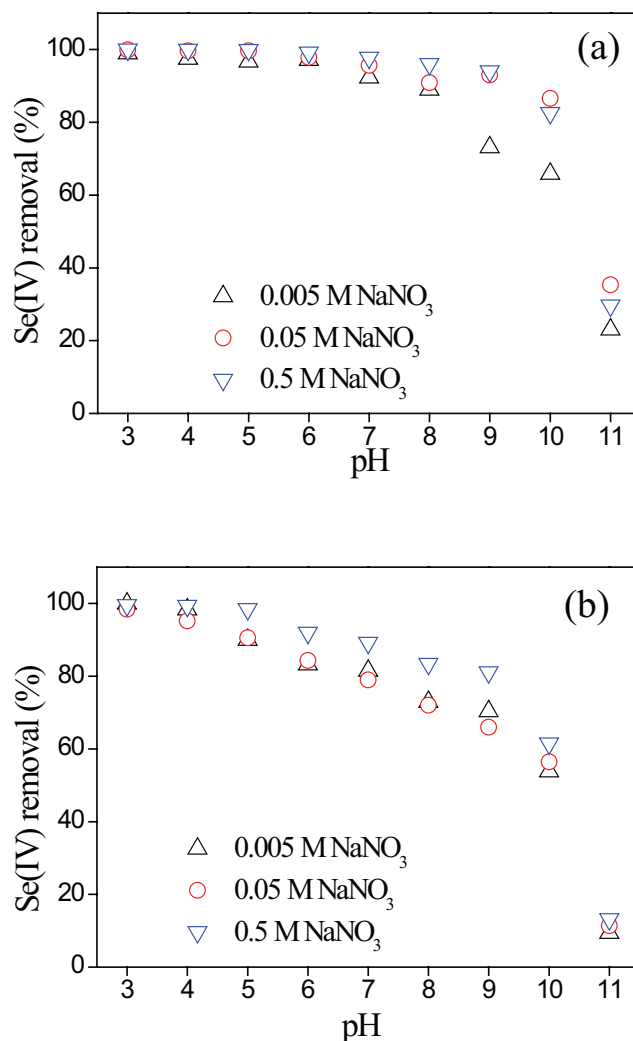


Fig. 3. Selenite sorption edges onto ^cFe–Mn (a) and ^mFe–Mn (b) at three different ionic strengths in NaNO₃ (0.005, 0.05 and 0.5 M). [Se(IV)] initial = 7.4 mg/L, adsorbent dose = 200 mg/L, T = 25°C ± 1°C.

^cFe–Mn and ^mFe–Mn have high Se(IV) sorption capacity and the former is much more effective for Se(IV) sorption than the latter. This suggests that Se(IV) sorption performance of the Fe–Mn binary oxide is significantly influenced by preparation method. Both Freundlich and Langmuir models were used to describe the experimental data of sorption isotherms. The Freundlich equation is represented as follows:

$$q_e = K_f C_e^n \quad (3)$$

where q_e is the amount of selenite adsorbed on the solid phase (mg/g), C_e is the equilibrium selenite concentration in solution phase (mg/L), K_F is roughly an indicator of the adsorption capacity and n is the heterogeneity factor which has a lower value for more heterogeneous surfaces.

The Langmuir equation can be written in the following form:

$$q_e = \frac{q_{\max} b C_e}{1 + b C_e} \quad (4)$$

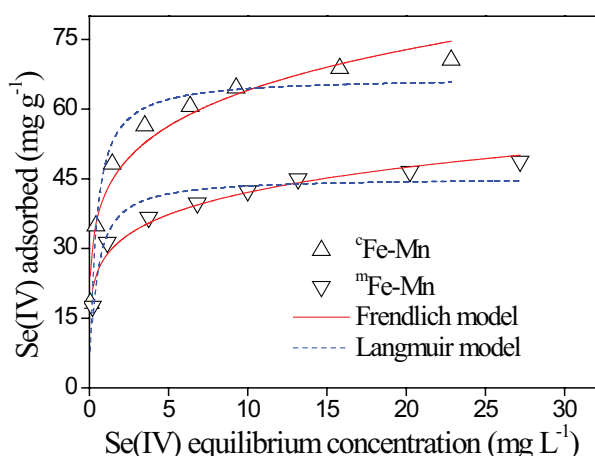


Fig. 4. Sorption isotherms of Se(IV) on ̑Fe-Mn and ̓Fe-Mn at pH 7.0 ± 0.1 and $T = 25^\circ\text{C} \pm 1^\circ\text{C}$.

Table 2

Langmuir and Freundlich isotherm parameters for Se(IV) adsorption on Fe–Mn binary oxide at pH 7.0 ± 0.1

Adsorbent	Langmuir model			Freundlich model		
	q_m (mg/g)	K_L (L/mg)	R^2	K_F (mg/g)	n	R^2
̓Fe-Mn	45.3	2.39	0.897	28.2	0.173	0.961
̑Fe-Mn	66.8	2.63	0.906	41.8	0.185	0.959

Table 3

Comparison of maximum selenite adsorption capacities for different adsorbents

Adsorbent	Equilibrium Se(IV) concentration range (mg/L)	pH	Maximum Se(IV) sorption capacity (mg/g)	Ref
̑Fe-Mn	0–30	7.0	70.5	Present study
̓Fe-Mn	0–30	7.0	48.6	Present study
Fe–Mn hydrous oxide	0–500	6.0	29.0	[23]
WMNLR	0–100	5.0	54.6	[43]
Fe–GAC	0–1.4	5.0	2.5	[15]
FeOOH	0–8	5.0	26.3	[5]
Nano-TiO ₂	0–16	5.0	7.7	[19]
AICB	0–8	6.7	11.1	[44]
Nano-Al ₂ O ₃	0–8	6.0	10.9	[44]

where q_e and C_e are previously denoted, b is the equilibrium adsorption constant related to the affinity of binding sites (L/mg) and q_{\max} is the maximum amount of the selenite per unit weight of adsorbent for complete monolayer coverage.

Table 2 lists the sorption constants obtained from the isotherms. Obviously, the experimental data are better fitted by Freundlich model than Langmuir model, with high correlation coefficients ($R^2 > 0.95$). The Langmuir isotherm assumes that sorption occurs on a homogeneous surface, while Freundlich equation describes adsorption where the adsorbent has a heterogeneous surface with adsorption sites that have different energies of adsorption [24]. For the Fe–Mn binary oxide systems, the presence of manganese dioxide in the adsorbent might result in a heterogeneous surface, especially for the ̓Fe-Mn . Consequently, the Langmuir isotherm fails to describe the sorption behavior of Se(IV) on the Fe–Mn binary oxides. The estimated maximal sorption capacity of Se(IV) on the ̓Fe-Mn and ̑Fe-Mn is 48.6 and 70.5 mg/g, respectively. In addition, the n value for ̓Fe-Mn is less than that of ̑Fe-Mn , indicating that the former has a more heterogeneous surface. The higher Se(IV) sorption capacity of ̑Fe-Mn may be due to its larger surface area. A comparison has been made between the prepared Fe–Mn binary oxide and previously reported sorbents for selenite sorption (Table 3). It can be seen that the ̑Fe-Mn outperforms remarkably many other sorbents, suggesting that the ̑Fe-Mn is a rather promising alternative for selenite removal.

3.5. Effect of co-existing anions

Anions such as chloride, fluoride, sulfate, bicarbonate, silicate and phosphate are generally present in the natural waters, and could compete with selenite for sorptive sites. The effects of these anions at three concentration levels (0.1, 1.0 and 5 mM) on selenite sorption were therefore examined at pH 7.0 ± 0.1 .

Fig. 5 shows the experimental results. For the ̑Fe-Mn , the co-existing chloride, fluoride and bicarbonate have no significant influence on Se(IV) sorption. The present sulfate slightly decreases the Se(IV) removal, whereas the co-existing silicate and phosphate suppress greatly the Se(IV) sorption, particularly at high concentration level. Truche et al. [45] observed

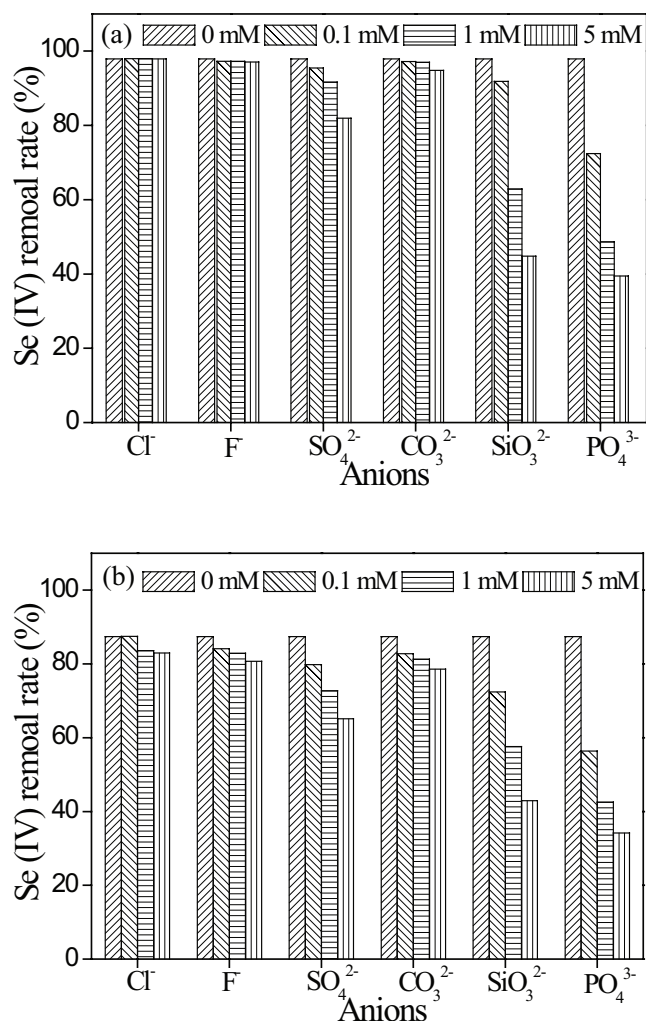


Fig. 5. Effects of co-existing anions on Se(IV) sorption onto α -Fe-Mn (a) and γ -Fe-Mn (b). [Se(IV)] initial = 0.094 mmol/L, adsorbent dose = 200 mg/L, pH = 7.0 \pm 0.1, T = 25°C \pm 1°C.

similar phenomenon when they studied nitrate sorption to stainless steels. Sulfate has no impact on the nitrate sorption while phosphate significantly hindered nitrate sorption. S and Se are located in the same main group in element periodic table, and the structure of sulfate ion is similar to that of selenite ion. The structures of silicate and phosphate are also close to selenite. Thus, the present sulfate, silicate and phosphate ions inevitably compete with selenite ions for adsorptive sites on the surface of Fe-Mn binary oxide. For the γ -Fe-Mn, similar phenomenon was observed.

From above, it is concluded that the sorption behavior of Se(IV) on the γ -Fe-Mn is very similar to that of the α -Fe-Mn, except that the latter exhibits a higher Se(IV) sorption capacity. Therefore, the investigations are focused on the Se(IV) sorption onto the surfaces of the α -Fe-Mn in the following sections.

3.6. Zeta potential measurement

The zeta potentials of the α -Fe-Mn before and after Se(IV) sorption were measured and shown in Fig. S3.

The isoelectric point (IEP) (defined as the point at which the electrokinetic potential equals zero) of the α -Fe-Mn was found to be at pH 6.0. After reaction with Se(IV), this pH_{IEP} value decreased to about 4.4. Specific adsorption of anions makes the surface of oxides more negatively charged, which results in a shift of the isoelectric point of adsorbent to a lower pH value [46]. Specific adsorption rather than a purely electrostatic interaction is further confirmed from the drop of isoelectric point at the aqueous selenite/ α -Fe-Mn interface.

3.7. XPS analysis

To confirm the presence of selenium and determine the oxidation state of adsorbed Se, XPS spectra of the α -Fe-Mn before and after Se(V) sorption were collected. The survey spectra are depicted in Fig. 6(a). It can be obviously seen the presence of SeLMMa and Se3p peaks, which indicates the sorption of Se(IV) onto the solid surface of sorbent.

Fig. 6(b) demonstrates the Se3d core level of the α -Fe-Mn before and after the sorption of Se(IV). Obviously, a new Se3d peak appeared after Se(IV) sorption. The Se3d binding energy is found to be 59.1 eV. The values of binding energy of Se3d core level for Se(IV) and Se(VI) in Na_2SeO_3 and Na_2SeO_4 were reportedly 59.1 and 61.6 eV, respectively [47]. Thus, it can be deduced that the selenium species adsorbed on surface of the α -Fe-Mn remained as Se(IV) species. Namely, the oxidation state of Se(IV) is not changed during the adsorption process. Similar result was also observed for Se(IV) adsorption on the Fe-Mn hydrous oxide [23], in which the Se3d binding energy of adsorbed selenite was found to be 58.8 eV. In addition, Scott and Morgan [48] also found that Se(IV) was not oxidized to Se(VI) by pure birnessite at pH 7.0 until 96 h. They believed that the small driving force of the redox reaction between HSeO_3^- and $\delta\text{-MnO}_2(\text{s})$ makes it barely thermodynamically possible ($\Delta E^\circ = +0.004$ V). This indicates that the Fe-Mn binary oxide is hard to oxidize Se(IV) to Se(VI), in spite of containing MnO_2 . Furthermore, O(1s) narrow scans of the Fe-Mn binary oxide before and after selenite sorption were collected and shown in Fig. 6(c).

The O(1s) spectra are composed of three overlapped peaks of oxide oxygen (O^{2-}), hydroxyl (OH^-) and adsorbed water (H_2O). The spectra were fitted using a nonlinear least-square curve fitting program (XPSPEAK41 Software) and the fitting results are shown in Fig. 6(c) and Table S2. For origin α -Fe-Mn, the OH^- and O^{2-} species are dominant, occupying 51.43% and 45.28%, respectively. After selenite sorption, the percentage of OH^- decreased slightly (from 51.43% to 46.59%); correspondingly, the O^{2-} species became relatively more abundant (from 45.28% to 51.17%). This might be explained that the OH^- on the surface of the α -Fe-Mn was partially replaced by the HSeO_3^- and subsequently inner-sphere surface complexes were formed. Similar phenomenon was also observed by Wen et al. [49] when they studied arsenic sorption by ordered mesoporous iron manganese bimetal oxides.

From the above-mentioned results, it can be reasonably deduced that the FeOOH in the α -Fe-Mn system is mainly responsible for the uptake of selenite, not only because of its higher content but also because of its greater affinity for selenium than manganese dioxide [20]. The manganese dioxide

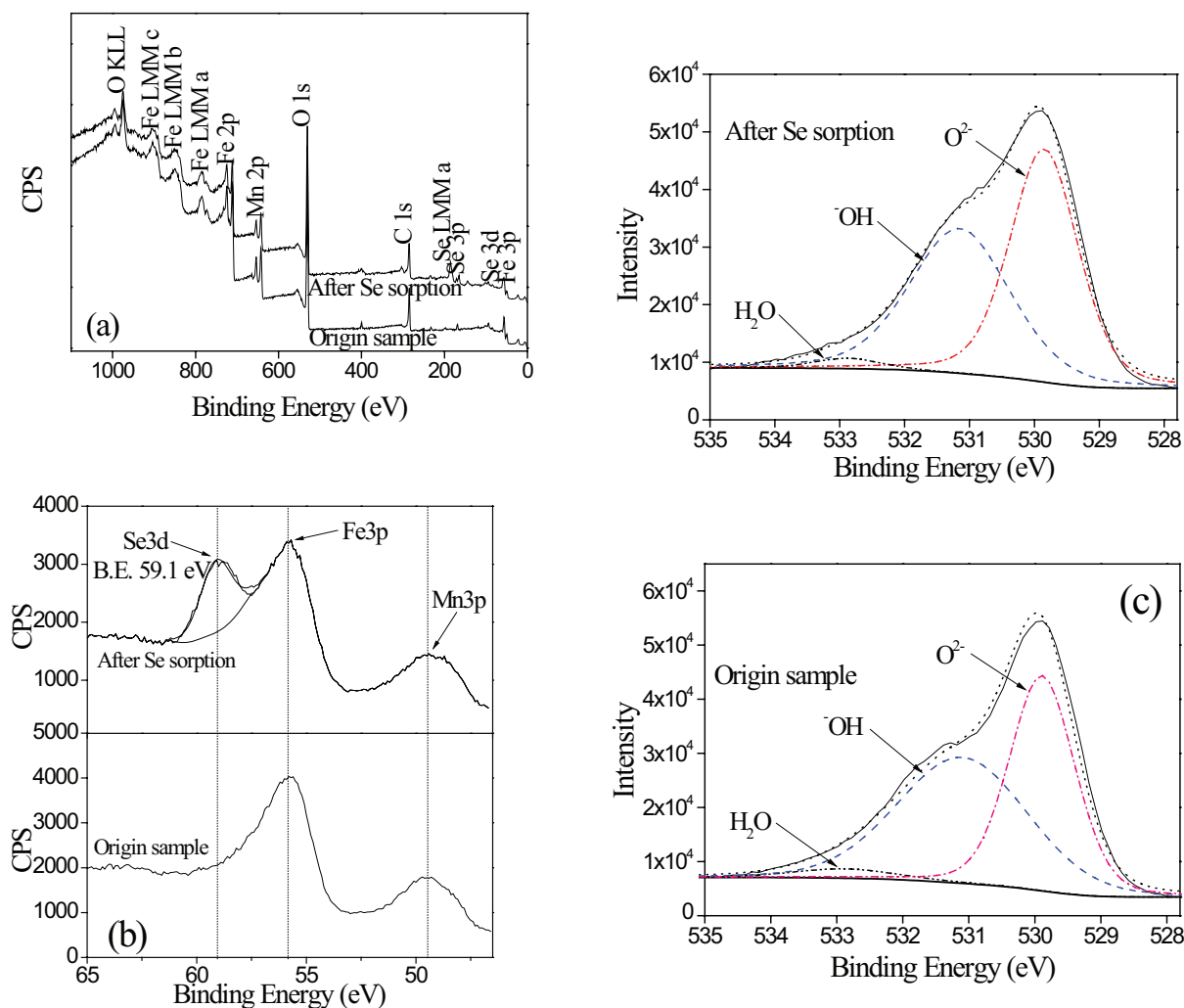


Fig. 6. XPS spectra of ⁴Fe–Mn before and after reaction with Se(IV). (a) Wide scan, (b) Se3d core level and (c) O(1s) spectra.

in the ⁴Fe–Mn system makes the particles smaller and thus results in a synergistic effect on selenite sorption.

4. Conclusions

Both ^mFe–Mn and ⁴Fe–Mn are amorphous and have similar structure to 2-line ferrihydrite. The ⁴Fe–Mn has a much higher specific BET surface than the ^mFe–Mn. The pseudo-second-order equation is more suitable to describe the kinetic data. Se(IV) sorption on both ^mFe–Mn and ⁴Fe–Mn is pH dependent, decreasing with an increase in pH value. The experimental data of isotherm are well fitted by the Freundlich model and the estimated maximal sorption capacity of Se(IV) on the ^mFe–Mn and ⁴Fe–Mn is 48.6 and 70.5 mg/g, respectively. The Fe–Mn binary oxide is able to adsorb selenite in the presence of competing anions and across a wide range of pH values. Among the co-existing anions, phosphate is the greatest competitor with selenite for adsorptive sites on the surface of oxide. Selenite is sorbed onto the surface of the Fe–Mn binary oxide by formation of inner-sphere surface complexes. The desirable properties of high sorption

capacity, low cost and environmental friendliness make Fe–Mn binary oxide a promising adsorbent for the removal of Se(IV) from water or wastewater.

Acknowledgment

The authors acknowledge the financial support by National Natural Science Foundation of China (Grant No. 51478457).

Symbols

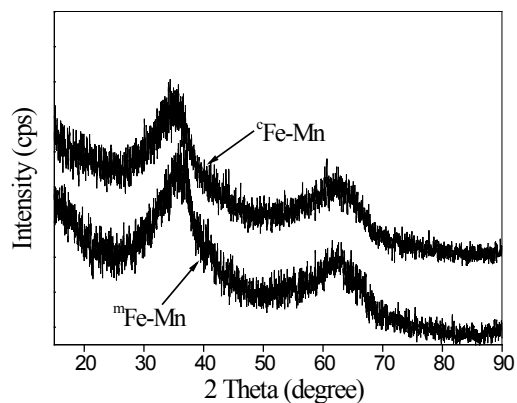
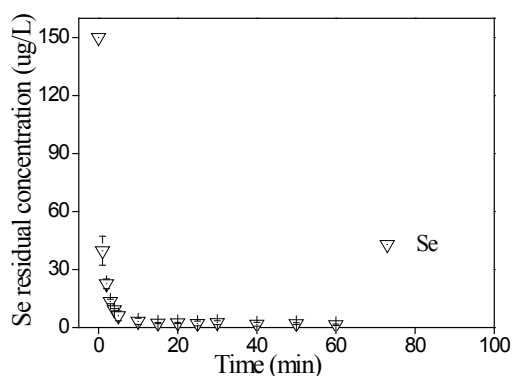
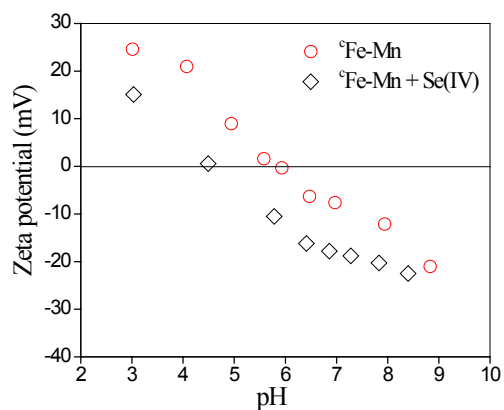
⁴ Fe–Mn	—	Fe–Mn binary oxide prepared by coprecipitation
^m Fe–Mn	—	Fe–Mn binary oxide prepared by mechanical mixing
XRD	—	X-ray diffraction
BET	—	Brunauer–Emmett–Teller
ICP–AES	—	Inductively coupled plasma atomic emission spectroscopy
IEP	—	Isoelectric point

References

- [1] S. Sharma, R. Singh, Selenium in soil, plant, and animal systems, *Crit. Rev. Environ. Control*, 13 (1984) 23–50.
- [2] F. Fordyce, Selenium geochemistry and health, *AMBIO*, 36 (2007) 94–97.
- [3] N. Jordan, A. Ritter, A.C. Scheinost, S. Weiss, D. Schild, R. Hübner, Selenium (IV) uptake by maghemite ($\gamma\text{-Fe}_2\text{O}_3$), *Environ. Sci. Technol.*, 48 (2014) 1665–1674.
- [4] S.J. Hamilton, Review of selenium toxicity in the aquatic food chain, *Sci. Total Environ.*, 326 (2004) 1–31.
- [5] M.O.M. Sharrad, H. Liu, M. Fan, Evaluation of FeOOH performance on selenium reduction, *Sep. Sci. Technol.*, 84 (2012) 29–34.
- [6] S.H. Hasan, D. Ranjan, M. Talat, Agro-industrial waste ‘wheat bran’ for the biosorptive remediation of selenium through continuous up-flow fixed-bed column, *J. Hazard. Mater.*, 181 (2010) 1134–1142.
- [7] M. Vinceti, C.M. Crespi, F. Bonvicini, C. Malagoli, M. Ferrante, S. Marmioli, S. Stranges, The need for a reassessment of the safe upper limit of selenium in drinking water, *Sci. Total Environ.*, 443 (2013) 633–642.
- [8] J. Torres, V. Pintos, S. Domínguez, C. Kremer, E. Kremer, Selenite and selenate speciation in natural waters: interaction with divalent metal ions, *J. Solution Chem.*, 39 (2010) 1–10.
- [9] K.H. Goh, T.T. Lim, Geochemistry of inorganic arsenic and selenium in a tropical soil: effect of reaction time, pH, and competitive anions on arsenic and selenium adsorption, *Chemosphere*, 55 (2004) 849–859.
- [10] B.J. Mariñas, R.E. Selleck, Reverse osmosis treatment of multicomponent electrolyte solutions, *J. Membr. Sci.*, 72 (1992) 211–229.
- [11] Y.W. Zhu, A.K. Sengupta, A. Ramana, Ligand exchange for anionic solutes, *React. Polym.*, 17 (1992) 229–237.
- [12] V. Mavrov, S. Stamenov, E. Todorova, H. Chmiel, T. Erwe, New hybrid electrocoagulation membrane process for removing selenium from industrial wastewater, *Desalination*, 201 (2006) 290–296.
- [13] L.P. Liang, W.J. Yang, X.H. Guan, J.L. Li, Z.J. Xu, J. Wu, Y.Y. Huang, X.Z. Zhang, Kinetics and mechanisms of pH-dependent selenite removal by zero valent iron, *Water Res.*, 47 (2013) 5846–5855.
- [14] N. Bleiman, Y.G. Mishael, Selenium removal from drinking water by adsorption to chitosan-clay composites and oxides: batch and columns tests, *J. Hazard. Mater.*, 183 (2010) 590–595.
- [15] C.-G. Lee, S.-B. Kim, Removal of arsenic and selenium from aqueous solutions using magnetic iron oxide nanoparticle/multi-walled carbon nanotube adsorbents, *Desal. Wat. Treat.*, 57 (2016) 28323–28339.
- [16] R. Kamaraj, S. Vasudevan, Decontamination of selenate from aqueous solution by oxidized multi-walled carbon nanotubes, *Powder Technol.*, 274 (2015) 268–275.
- [17] D. Peak, D.L. Sparks, Mechanisms of selenate adsorption on iron oxides and hydroxides, *Environ. Sci. Technol.*, 36 (2002) 1460–1466.
- [18] W.H. Kuan, S.L. Lo, M.K. Wang, C.F. Lin, Removal of Se (IV) and Se (VI) from water by aluminum-oxide-coated sand, *Water Res.*, 32 (1998) 915–923.
- [19] L. Zhang, N. Liu, L.J. Yang, Q. Lin, Sorption behavior of nano-TiO₂ for the removal of selenium ions from aqueous solution, *J. Hazard. Mater.*, 170 (2009) 1197–1203.
- [20] L.S. Balistrieri, T.T. Chao, Adsorption of selenium by amorphous iron oxyhydroxide and manganese dioxide, *Geochim. Cosmochim. Acta*, 54 (1990) 739–751.
- [21] C.M. Gonzalez, J. Hernandez, J.G. Parsons, J.L. Gardea-Torresdey, A study of the removal of selenite and selenate from aqueous solutions using a magnetic iron/manganese oxide nanomaterial and ICP-MS, *Microchem. J.*, 96 (2010) 324–329.
- [22] M. Martínez, J. Giménez, J. de Pablo, M. Rovira, L. Duro, Sorption of selenium(IV) and selenium(VI) onto magnetite, *Appl. Surf. Sci.*, 252 (2006) 3767–3773.
- [23] M. Szlachta, V. Gerda, N. Chubar, Adsorption of arsenite and selenite using an inorganic ion exchanger based on Fe–Mn hydrous oxide, *J. Colloid Interface Sci.*, 365 (2012) 213–221.
- [24] Z.M. Ren, G.S. Zhang, J.P. Chen, Adsorptive removal of arsenic from water by an iron–zirconium binary oxide adsorbent, *J. Colloid Interface Sci.*, 358 (2011) 230–237.
- [25] T. Basu, U.C. Ghosh, Nano-structured iron(III)–cerium(IV) mixed oxide: synthesis, characterization and arsenic sorption kinetics in the presence of co-existing ions aiming to apply for high arsenic groundwater treatment, *Appl. Surf. Sci.*, 283 (2013) 471–481.
- [26] Z.J. Li, S.B. Deng, G. Yu, J. Huang, V.C. Lim, As (V) and As (III) removal from water by a Ce–Ti oxide adsorbent: behavior and mechanism, *Chem. Eng. J.*, 161 (2010) 106–113.
- [27] J.B. Lǚ, H.J. Liu, R.P. Liu, X. Zhao, L.P. Sun, J.H. Qu, Adsorptive removal of phosphate by a nanostructured Fe–Al–Mn trimetal oxide adsorbent, *Powder Technol.*, 233 (2013) 146–154.
- [28] G.S. Zhang, J.H. Qu, H.J. Liu, R.P. Liu, R.C. Wu, Preparation and evaluation of a novel Fe–Mn binary oxide adsorbent for effective arsenite removal, *Water Res.*, 41 (2007) 1921–1928.
- [29] G.S. Zhang, J.H. Qu, H.J. Liu, R.P. Liu, G.T. Li, Removal mechanism of As (III) by a novel Fe–Mn binary oxide adsorbent: oxidation and sorption, *Environ. Sci. Technol.*, 41 (2007) 4613–4619.
- [30] G.S. Zhang, H.J. Liu, R.P. Liu, J.H. Qu, Removal of phosphate from water by a Fe–Mn binary oxide adsorbent, *J. Colloid Interface Sci.*, 335 (2009) 168–174.
- [31] W. Xu, H.J. Wang, R.P. Liu, X. Zhao, J.H. Qu, The mechanism of antimony (III) removal and its reactions on the surfaces of Fe–Mn binary oxide, *J. Colloid Interface Sci.*, 363 (2011) 320–326.
- [32] J.W. Murray, The surface chemistry of hydrous manganese dioxide, *J. Colloid Interface Sci.*, 46 (1974) 357–371.
- [33] U. Schwertmann, R.M. Cornell, *Iron Oxides in the Laboratory: Preparation and Characterization*, Wiley-VCH, Weinheim, 2000.
- [34] A. Hofmann, M. Pelletier, L. Michot, A. Stradner, P. Schurtenberger, R. Kretzschmar, Characterization of the pores in hydrous ferric oxide aggregates formed by freezing and thawing, *J. Colloid Interface Sci.*, 271 (2004) 163–173.
- [35] M.L. Pierce, C.B. Moore, Adsorption of arsenite and arsenate on amorphous iron hydroxide, *Water Res.*, 16 (1982) 1247–1253.
- [36] W. Stumm, *Chemistry of the Solid-Water Interface*, John Wiley & Sons, New York, 1992.
- [37] M. Rovira, J. Giménez, M. Martínez, X. Martínez-Lladó, J.D. Pablo, V. Martí, L. Duro, Sorption of selenium (IV) and selenium (VI) onto natural iron oxides: goethite and hematite, *J. Hazard. Mater.*, 150 (2008) 279–284.
- [38] N. Jordan, C. Lomenech, N. Marmier, E. Giffaut, J.J. Ehrhardt, Sorption of selenium (IV) onto magnetite in the presence of silicic acid, *J. Colloid Interface Sci.*, 329 (2009) 17–23.
- [39] W. Stumm, C.P. Huang, S.R. Jenkins, Specific chemical interaction affecting stability of dispersed systems, *Croat. Chem. Acta*, 42 (1970) 223–245.
- [40] M.B. McBride, A critique of diffuse double layer models applied to colloid and surface chemistry, *Clays Clay Miner.*, 45 (1997) 598–608.
- [41] M. Duc, G. Lefevre, M. Fedoroff, J. Jeanjean, J.C. Rouchaud, F. Monteil-Rivera, J. Dumonceau, S. Milonjic, Sorption of selenium anionic species on apatites and iron oxides from aqueous solutions, *J. Environ. Radioact.*, 70 (2003) 61–72.
- [42] C.M. Su, D.L. Suarez, Selenate and selenite sorption on iron oxides an infrared and electrophoretic study, *Soil Sci. Soc. Am. J.*, 64 (2000) 101–111.
- [43] S.S. Dash, K.M. Parida, Studies on selenite adsorption using manganese nodule leached residues, *J. Colloid Interface Sci.*, 307 (2007) 333–339.
- [44] J.S. Yamani, A.W. Lounsbury, J.B. Zimmerman, Adsorption of selenite and selenate by nanocrystalline aluminum oxide, neat and impregnated in chitosan beads, *Water Res.*, 50 (2014) 373–381.
- [45] L. Truche, G. Berger, A. Albrecht, L. Domergue, Engineered materials as potential geocatalysts in deep geological nuclear waste repositories: a case study of the stainless steel catalytic effect on nitrate reduction by hydrogen, *Appl. Geochem.*, 35 (2013) 279–288.

- [46] T.H. Hsia, S.L. Lo, C.F. Lin, D.Y. Lee, Characterization of arsenate adsorption on hydrous iron oxide using chemical and physical methods, *Colloids Surf., A*, 85 (1994) 1–7.
- [47] D.S. Han, B. Batchelor, A. Abdel-Wahab, XPS analysis of sorption of selenium (IV) and selenium (VI) to mackinawite (FeS), *Environ. Prog. Sustainable Energy*, 32 (2013) 84–93.
- [48] M.J. Scott, J.J. Morgan, Reactions at oxide surfaces. 2. Oxidation of Se (IV) by synthetic birnessite, *Environ. Sci. Technol.*, 30 (1996) 1990–1996.
- [49] Z.P. Wen, Y.L. Zhang, C.M. Dai, B. Chen, S.J. Guo, H. Yu, D.L. Wu, Synthesis of ordered mesoporous iron manganese bimetal oxides for arsenic removal from aqueous solutions, *Microporous Mesoporous Mater.*, 200 (2014) 235–244.
- [50] G.S. Zhang, H.J. Liu, R.P. Liu, J.H. Qu, Adsorption behavior and mechanism of arsenate at Fe–Mn binary oxide/water interface, *J. Hazard. Mater.*, 168 (2009) 820–825.

Supplementary information

Fig. S1. XRD patterns of $\bar{\epsilon}$ Fe-Mn and \bar{m} Fe-Mn.Fig. S2. Sorption kinetic of Se(IV) on $\bar{\epsilon}$ Fe-Mn at low initial concentration. [Se(IV)] initial = 150 μ L, adsorbent dose = 200 mg/L, pH = 7.0 \pm 0.1, T = 25°C \pm 1°C.Fig. S3. Zeta potential of $\bar{\epsilon}$ Fe-Mn before and after Se(IV) sorption. [Se(IV)] initial = 10 mg/L, adsorbent dose = 200 mg/L, equilibrium time = 72 h, T = 25°C \pm 1°C.Table S1
BET specific surface area and porosity measurements of different adsorbents

Adsorbent	Specific surface area ($\text{m}^2 \text{g}^{-1}$)	Average pore diameter (\AA)	Average pore volume ($\text{cm}^3 \text{g}^{-1}$)
FeOOH ^a	247	40	0.25
MnO ₂	121	109	0.33
\bar{m} Fe-Mn	219	42	0.23
$\bar{\epsilon}$ Fe-Mn ^a	265	71	0.47

^aThe data has been published in our previous study [50].Table S2
O(1s) peak parameters for $\bar{\epsilon}$ Fe-Mn before and after selenite sorption

Sample	Peak ^a	B. E. (eV)	Percent (%) ^b
$\bar{\epsilon}$ Fe-Mn	O ²⁻	529.89	45.28
	OH ⁻	531.10	51.43
	H ₂ O	532.88	3.29
$\bar{\epsilon}$ Fe-Mn-Se	O ²⁻	529.85	51.17
	OH ⁻	531.15	46.59
	H ₂ O	532.88	2.24

^aSurface species: O²⁻: oxygen bonded to metal; OH⁻: hydroxyl bonded to metal; H₂O: sorbed water.^bThe percentage represents the contribution of each peak to the total amount of the O(1s) peak.